Proceedings of the Eighth International Conference on Computational Structures Technology
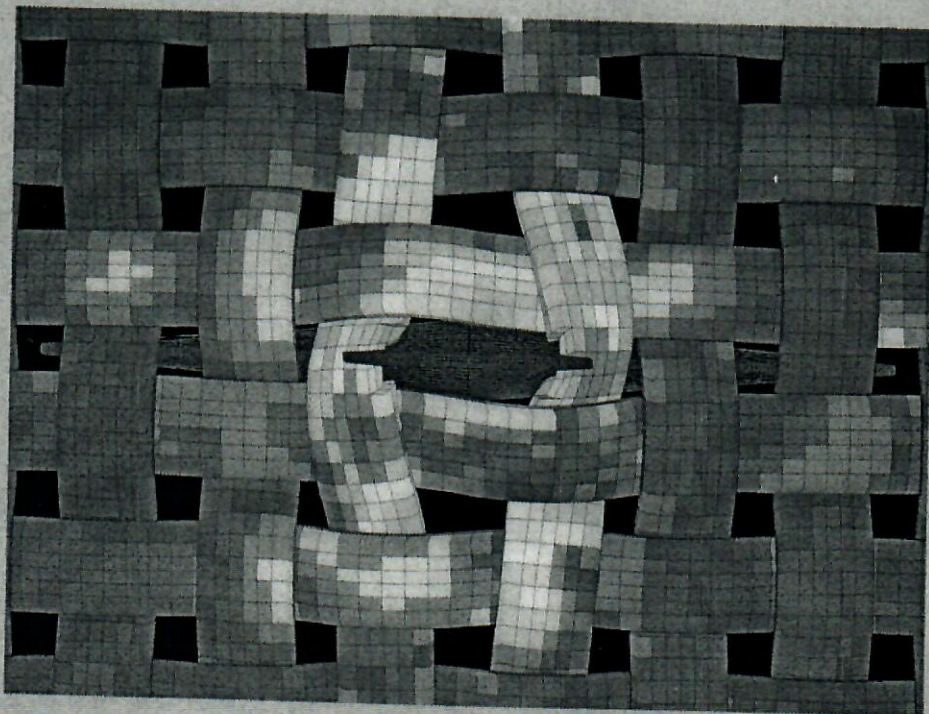
Edited by
B.H.V. Topping, G. Montero and R. Montenegro

Las Palmas de Gran Canaria - Spain
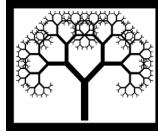12-15 September 2006

CIVIL-COMP PRESS

Cover Image: Yarn failure and element stress distributions during simulation of knife penetration into a woven fabric. This image is used with the permission of W.M. Gao. For more details, see Paper 90.

Contents

Paper 99

Modelling Frequency Adjustment Effects Using Shape Memory Alloy Oscillators

L.X. Wang† and R.V.N. Melnik‡
† MCI, Faculty of Science and Engineering
  University of Southern Denmark, Sonderborg, Denmark
‡ Mathematical Modelling and Computational Sciences
  Wilfrid Laurier University, Waterloo ON, Canada

Abstract

Mechanical vibrations constitute a common phenomenon in applications of many engineering structures and systems. Such vibrations should often be tuned according to a specific application. In many application developments, a supplementary oscillator with a suitable frequency is attached to the primary system, by which the primary vibration can be tuned. For the cases where the primary vibration frequency is uncertain, it is always beneficial to make a supplementary vibration frequency continuously variable in a rather wide range. In other cases, when the excitation might not be a mono-frequency or harmonic, or the frequency drifts, the vibration absorber is expected to be robust and still be able to tune the vibration at some extent.

In the present paper, we model the performance of a shape memory alloy oscillator used as a vibration absorber. It consists of a shape memory alloy rod and an end-mass. The vibration characteristic of the oscillator is continuously adjustable by changing its temperature, due to the thermo-mechanical coupling property of the shape memory alloy rod. In addition, the first order phase transformation in the SMA rod at low temperatures also contributes robustly to vibration attenuation, due to hysteresis induced. This is can be used for the cases where the vibration and excitation frequencies are unknown, or drift. The dynamic response of the SMA oscillator is modeled by a nonlinear partial differential equation using the modified Ginzburg-Landau theory. This model is then simplified to a nonlinear model convenient for the vibration analysis.

Since the SMA oscillator has a very strong nonlinearity, its frequency response is not obtainable in analytical form. We use numerical simulation tools to evaluate its performance. It is demonstrated that the SMA oscillator is able to tune the vibration of the primary system within a rather wide frequency range. The performance of the SMA oscillator is close to a regular linear oscillator at high temperature when only the austenite phase exists. The vibration attenuation of the SMA oscillator at low temperature exhibits a more complicated behaviour induced by the hysteresis effects in the SMA rod.

Keywords: vibration tuning, frequency adjustment, shape memory alloys, hysteresis.

1

1 Introduction

Forced vibrations have been investigated for centuries. Nevertheless, as centuries ago, they bring along such consequences as noise, resonance, structure failure, and dealing with these consequences still represents a problem at the forefront of modern science and engineering. In many engineering applications, it is desirable to attenuate or completely suppress the vibrations. Among many approaches, the dynamical vibration absorber is a popular and simple tool for this purpose. The principle of the dynamical vibration absorber is to absorb vibration energy from the primary system and store it in the attached vibration absorber, via its own vibrations, which will reduce the vibration of the primary system as a consequence [5, 7]. When the excitation frequency is close to the natural frequency of the primary system, and is known, the dynamical vibration absorber can be easily implemented by a linear mass-spring oscillator, as sketched in the left part of Figure (1), and be able to suppress the vibration of the primary system completely.

The limitation of the linear mass-spring oscillator used as a vibration absorber is that it only works when the excitation frequency is known and close to (or ideally equal to) the natural frequency of the primary system. For many engineering structures, both of them might be uncertain [5, 7]. For these cases, adaptive oscillators with adjustable stiffness are sought to tune the vibration, so the natural frequency of the oscillator can be adjusted to match the resonance frequency of the primary system. Due to its thermo-mechanical coupling properties, Shape Memory Alloys (SMAs) are promising materials used for adaptive vibration absorbers [4, 14, 15]. The unique properties of the SMAs is that the material will be in the austenite phase at higher temperature, with hardened elastic modulus, while at lower temperature, the material will be in the martensite phase and much softer. When the temperature is continuously adjusted, its elastic modulus will be also changing. The thermo-mechanical coupling properties of SMAs provide a way to adjust the frequency response of vibration absorbers for adaptive vibration tuning [8, 10, 11]. There have been a number of publications on the SMA (composite) beams used as vibration absorbers, and it has been shown that the frequency of the oscillator using the SMA beam can be adjusted in a range of 15% percent [4, 14, 15]. For the reported applications, only the thermo-mechanical coupling property of the SMA material has been used.

If one considers the vibration tuning for more realistic cases where the excitation might not be mono-frequency or harmonic, and the primary system itself might be a nonlinear system, the adaptive vibration absorber designed according to frequency analysis might not be a suitable choice. Indeed, the vibration tuning procedure should be implemented in a general way by taking into account energy dissipation. For this purpose, another property of SMAs can be used, namely the hysteresis induced by the first order martensitic phase transformations at low temperature [1]. As we mentioned earlier, the SMA is in the martensite phase at low temperature, and the material can be switched between two martensite variants by external loadings in the one dimensional case, during which the external energy input into the material will be dissipated without residual displacement after unloading [15]. Some investigations have already

been carried out to understand the damping effects of SMAs [2, 6, 8, 9]. In most cases, the constitutive laws were approximated by linear combinations related to damping effects pertinent to different phases which limits the applicability of the associated PDE-based models, in particular for the analysis of vibration tuning.

In order to exploit the application potential of SMA materials in vibration tuning, in this paper both aspects of the SMA properties, thermo-mechanical coupling and phase-transformation-induced hysteresis, are taken into account and are used simultaneously. In particular, we employ an idealized SMA rod with an end-mass as a vibration absorber. For the vibration analysis, the SMA rod can be modeled as a nonlinear spring with adjustable stiffness. At the same time, hysteresis might also be induced at low temperature. In order to better capture the thermo-mechanical coupling and nonlinear nature of the constitutive law of the SMA oscillator, the modified Ginzburg- Landau theory is employed to model the dynamic response of the SMA rod [3, 6, 13]. The problem is reduced to a nonlinear algebraic equation which gives the force-deformation relation of the oscillator. Vibration tuning is then analyzed using this simplified model for various cases.

2 Nonlinear Vibrations
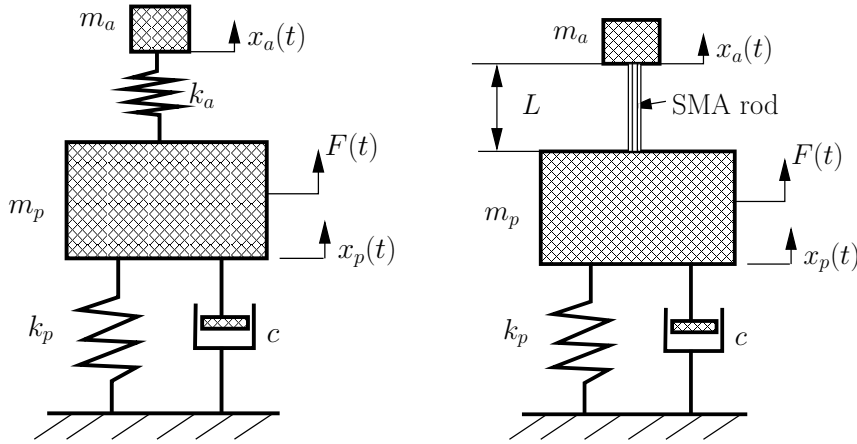
Figure 1: Sketch of dynamic vibration absorbers. Left: A linear mass vibration absorber. Right: A shape memory alloy based vibration absorber.

The principle of applying a SMA oscillator as a vibration absorber is very similar to that of a linear oscillator, as sketched in Figure (1). The oscillator still consist of an elastic component and an attached end-mass. In the SMA oscillator, the elastic component is replaced by a SMA rod. We assume that we only consider idealized situation here, where we are able to adjust the length and cross-section area of the SMA rod as needed, without worrying about structure design, buckling effect,etc.

To model the vibration tuning, the vibration of the primary system and the attached

oscillator should be considered simultaneously. To do so, let us formulate the governing equation of the entire system based on the Newton's law as follows:

$$
\begin{aligned}
m_p \ddot{x}_p \;\; + \;\; & c_p \dot{x}_p + k_p x_p - F_s(x_p - x_a) = F(t), \\
m_a \ddot{x}_a \;\; = \;\; & F_s(x_p - x_a),
\end{aligned}
\tag{1}
$$

where x_p and x_a are displacements of the primary and attached mass blocks, m_p and m_a, respectively; c_p is the friction coefficient and k_p is the spring stiffness in the primary system. The primary system is subject to an excitation input $F(t)$ which might be decomposed into various harmonic components. The nonlinear restoring force produced by the SMA rod is denoted by F_s, a general nonlinear function of deformation $x_p - x_a$ in the above equation. This model is easily generalizable by replacing the linear spring restoring force $k_p x_p$ for a nonlinear one.

If both the restoring forces in the primary system and the attached oscillator are linear, which is the case in the left part of Figure 1, the displacement x_p can be obtained by following the standard methodology and using the following transfer function:

$$
\frac{X_p(j\omega)}{F(j\omega)} = \frac{k_a - m_a\omega^2}{(-m_p\omega^2 + jc_p\omega + k_p + k_a)(-m_a\omega^2 + k_a) - k_a^2},
\tag{2}
$$

where ω is the frequency of the mono-frequency excitation force. If ω is close or equal to the natural frequency of the primary system, it will induce resonance. The vibration absorber can be designed to completely suppress the vibration by setting the modulus of the transfer function to zero, which can be obtained by setting $k_a = m_a\omega^2$.

3 Dynamics of Shape Memory Alloy Oscillators

To model the nonlinear restoring force from the SMA rod, we start from the model which is able to capture thermo-mechanical coupling effect and the first order phase transformations in the material. For this purpose, the modified Ginzburg - Landau theory is employed here in a way similar to [3, 6, 13]. The coupling between thermal and mechanical fields in the Ginzburg-Landau theory is double-directional, which means that the mechanical oscillation will induce temperature oscillations, as well as that the temperature change will induce mechanical response. But for the purpose of the current analysis, the temperature of the material is considered as a tool to adjust its stiffness and it is assumed to be controlled to a specific value for a specific vibration frequency. Therefore, the thermal field can be neglected in such an analysis and only the mechanical field needs to be considered. Nevertheless, it should be coupled with the material temperature intrinsically.

To account for the dynamics of the mechanical field, the Lagrangian $\mathcal{L}$ for the SMA material is introduced as the sum of kinetic and potential energy contributions:

$$
\mathcal{L} = \frac{\rho}{2}(\dot{u})^2 - \mathcal{F},
\tag{3}
$$

where ρ is the density of the material and u is the displacement of particles in the SMA rod; $\mathcal{F}$ is the potential energy density of the material stored via deformations. The important feature of the Ginzburg - Landau theory is that the potential energy density is constructed as a non-convex function of the chosen *order parameters* and temperature θ. It can be formulated as a sum of the local energy density ($\mathcal{F}_l$) and the non-local energy density ($\mathcal{F}_g$). For the current one-dimensional problem, the strain $\varepsilon(x,t) = \frac{\partial u}{\partial x}$ is chosen as the order parameter, and the local free energy density can be constructed as the Landau free energy density $\mathcal{F}_l(\theta, \varepsilon)$ [3, 13]:

$$\mathcal{F}_l(\theta, \varepsilon) = \frac{k_1(\theta - \theta_1)}{2}\varepsilon^2 + \frac{k_2}{4}\varepsilon^4 + \frac{k_3}{6}\varepsilon^6, \tag{4}$$

where k_1, k_2, and k_3 are material-specific constants, θ_1 is the reference transformation temperature, which is also a material specific constant.

The non-local free energy density is usually constructed in a way similar to the class of ferroelastic materials as follows [3]:

$$\mathcal{F}_g(\nabla\varepsilon) = k_g(\frac{\partial\varepsilon}{\partial x})^2, \tag{5}$$

where k_g is a material-specific constant. The non-local term above accounts for inhomogeneous strain field. It represents energy contributions from domain walls of different phases. In order to account for dissipation effects of the accompanying phase transformations, a Rayleigh dissipation term can be introduced as follows:

$$\mathcal{F}_R = \frac{1}{2}\nu(\frac{\partial\varepsilon}{\partial t})^2, \tag{6}$$

where ν is a material-specific constant. The dissipation term accounts for the internal friction accompanying the movement of the interfaces between different phases. At macro-scale, it will be translated into the viscous effects of phase transformations [3, 12].

By substituting the potential energy density into the Lagrangian function given in Equation.(3), and minimizing the total energy with respect to the displacement field $u(x,t)$ according to the Hamilton principle:

$$\delta\int_0^T\int_0^L \mathcal{L}dtdx = \delta\int_0^T\int_0^L \left(\frac{\rho}{2}(\dot{u})^2 - \mathcal{F}\right)dtdx = 0, \tag{7}$$

we can obtain the governing equation for the dynamics of the mechanical field can be obtained and, provided that the dissipation effects are also taken into account, they can be given as follows:

$$\rho\ddot{u} = \frac{\partial}{\partial x}\left(k_1(\theta - \theta_1)\varepsilon + k_2\varepsilon^3 + k_3\varepsilon^5\right) + \nu\frac{\partial}{\partial t}\frac{\partial^2 u}{\partial x^2} - k_g\frac{\partial^4 u}{\partial x^4}. \tag{8}$$

This can be reduced to the following differential algebraic form together with stress boundary conditions:

$$\rho \ddot{u} = \frac{\partial \sigma}{\partial x} + \nu \frac{\partial}{\partial t} \frac{\partial^2 u}{\partial x^2} - k_g \frac{\partial^4 u}{\partial x^4},$$
$$\sigma = k_1(\theta - \theta_1)\varepsilon + k_2 \varepsilon^3 + k_3 \varepsilon^5, \tag{9}$$
$$\sigma(0) = \sigma_L, \;\; \sigma(L) = \sigma_R,$$

where σ is the stress in the SMA rod, σ_L and σ_R are given boundary stresses, L is the length of the SMA rod. Here we implicitly assumed that the two ends of the rod are at $x = 0$ and $x = L$, respectively.

The dependency of the dynamics of the mechanical field on the temperature is included in the above formulation. It has been shown that the above model is able to capture the thermo-mechanical coupling effect and the first order phase transformations in SMA rod [3, 13]. The difficulty in applying the above model in the analysis of vibration absorption is that the numerical simulation of the dynamic response of the system is not trivial [6, 13]. The simulation of the phase transformations and wave propagations in the SMA rod is a computationally expensive problem. For the current problem, phase transformations and wave propagations in the SMA rod (on the order of the speed of sound) are much faster than the vibration speed of the mass blocks. Hence, for the vibration analysis, the phase transformation process and wave propagation process can be neglected, and only the steady counterpart of Equation (9) is needed.

With the above observation, we can set all the time derivative terms in Equation (9) to zero. The simplification yields the following relation:

$$\sigma = k_1(\theta - \theta_1)\varepsilon + k_2 \varepsilon^3 + k_3 \varepsilon^5, = k_g \frac{\partial^2 \varepsilon}{\partial x^2} \;\; \sigma(0) = \sigma_L, \;\; \sigma(L) = \sigma_R. \tag{10}$$

Because we are interested in the SMA rod as a nonlinear spring and will be modelled a lumped system, the above relation can be further simplified by assuming that the strain distribution in the SMA rod is uniform, so that $\varepsilon = \Delta L / L$. We neglect the mass of the SMA rod since it is much smaller than the mass block m_a, so that the force-deformation relation for the SMA rod can be re-cast as follows:

$$F_s = \beta \left(k_1(\theta - \theta_1)\frac{\Delta L}{L} + k_2 \left(\frac{\Delta L}{L}\right)^3 + k_3 \left(\frac{\Delta L}{L}\right)^5 \right), \tag{11}$$

where β is the cross-section area of the SMA rod and ΔL is the deformation due to the force. By choosing appropriate β and L values, and assuming that one end of the SMA rod is fixed on the primary mass block while another on the attached block, we are able to formulate the restoring force as the follows:

$$F_s = K_1 \Delta\theta(x_p - x_a) + K_2(x_p - x_a)^3 + K_3(x_p - x_a)^5, \tag{12}$$

where the definition of K_1, K_2 and K_3 are obvious from the above equation. It is shown that the restoring force is dependent on the temperature, due to the thermo-mechanical coupling effect. At the same time, the hysteresis due to the first order

6

phase transformations is also captured in this model. If the internal viscosity of the SMA rod is also taken into account, the term $\nu \frac{\partial}{\partial t} \frac{\partial^2 u}{\partial x^2}$ in Equation (8) should not be set to zero, in which case F_s will not be a pure elastic force, but a combination of forces:

$$F_s = K_1 \Delta \theta (x_p - x_a) + K_2 (x_p - x_a)^3 + K_3 (x_p - x_a)^5 + c_\nu (\dot{x}_p - \dot{x}_a), \qquad (13)$$

where the contribution of friction force $c_\nu (\dot{x}_p - \dot{x}_a)$ plays of a similar role to the term $c_p \dot{x}_p$ in the primary system. For illustration of frequency adjustability, the friction force of the SMA oscillator is neglected in what follows next.

The model for the SMA rod given in Equation (12) is nonlinear. For convenience of the analysis, we introduce an equivalent stiffness K_e for the SMA rod, which leads to the following difference minimized:

$$\int_{x_b}^{x_t} (F_s (x_p - x_a) - F_a (x_p - x_a))^2 dx, \qquad (14)$$

where $F_s (x_p - x_a)$ is the restoring force calculated using Equation (12) and $F_a (x_p - x_a) = K_e (x_p - x_a)$ is the linear approximation that is calculated by using the equivalent stiffness; x_b and x_t are the minimal and maximal values of $x_p - x_a$, which are chosen before the simulation. It is obvious that the estimated K_e also depends on the choice of x_b and x_t.

To illustrate the dependence of the equivalent stiffness of the SMA rod on temperature, the force-deformation relations given in Equation (12) are plotted for the material $Au_{23}Cu_{30}Zn_{47}$ with four different temperatures (solid curves), together with those estimated equivalent stiffness (dashed straight lines). The SMA rod length is chosen $4m$ with cross-section area $\beta = 3.83 \times 10^{-5} m^2$. The details of the parameters for the chosen materials are listed in Table (1). The hysteresis is well pronounced when $\theta = 210\ K$, as indicated by the dashed lines with arrows, in the sub-plot (a). It is worth to note that the force-deformation relation given in Equation (12) is not linearizable, especially at low temperature, because it is not structure stable. At high temperature, the behaviour of SMA rod is very close to a linear spring, but with its stiffness linearly dependent on its temperature.

4 Numerical Results

Using Equation (12) for the nonlinear restoring force of the SMA oscillator, the governing equation for the primary and attached system can be formulated finally as follows:

$$\begin{aligned}
m_p \ddot{x}_p &+ c_p \dot{x}_p + k_p x_p - K_1 \Delta \theta (x_p - x_a) + K_2 (x_p - x_a)^3 + K_3 (x_p - x_a)^5 = F(t), \\
m_a \ddot{x}_a &= K_1 \Delta \theta (x_p - x_a) + K_2 (x_p - x_a)^3 + K_3 (x_p - x_a)^5.
\end{aligned} \qquad (15)$$

Using this model, the vibration of the primary and attached blocks can be simulated simultaneously, and the information on their velocities can also be extracted. The
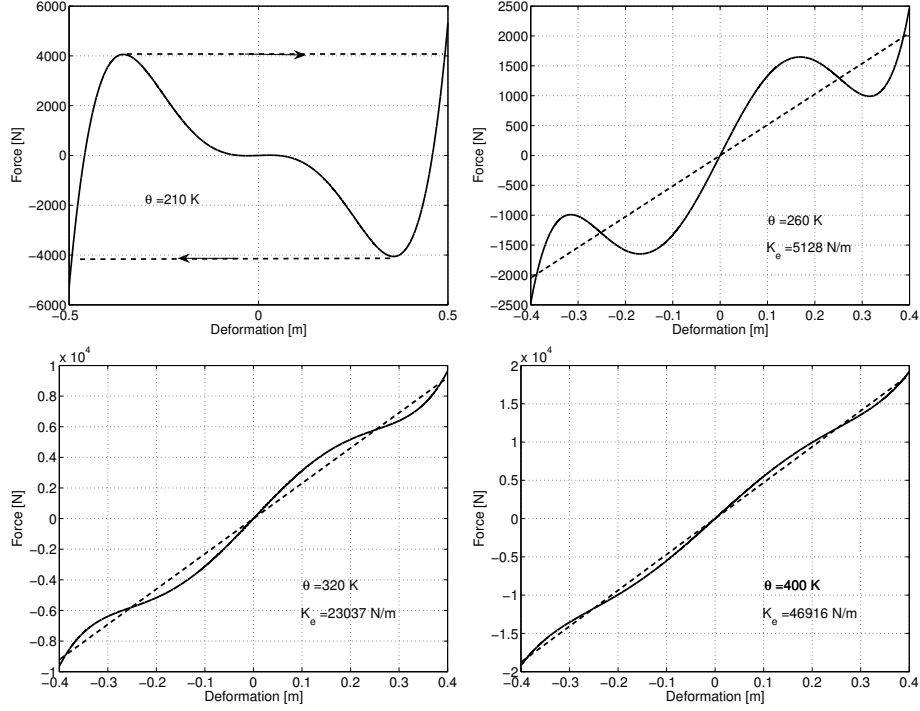
Figure 2: Sketch of the force-deformation relation of a shape memory alloy rod. From left to right, top to bottom, (a) $\theta = 210K$, (b) $\theta = 260K$, (c) $\theta = 320K$, (d) $\theta = 400K$.

parameters for the numerical simulation are listed in Table (1), from which the natural frequency of the primary system can be easily calculated as $\omega_n = \sqrt{k_p/m_p} = 80 \ rad/s$.

Parameter	Value		Parameter	Value
m_p	$10 \ k_g$		k_p	$64000 \ N/m$
m_a	$5 \ k_g$		c_p	$100 \ Ns/m$
t_0	0 s		t_f	10 s
θ_0	208 K		k_1	$4.8 \times 10^7 \ kg/s^2mK$
k_2	$6.0 \times 10^{11} \ kg/s^2m$		k_3	$8.0 \times 10^{13} \ kg/s^2m$
β	$3.83 \times 10^{-5}m^2$		L	$4 \ m$

Table 1: Computational parameters of the shape memory alloy vibration absorber.

For the illustration purpose, we first employ an excitation force with a mono-frequency, which is equal to the natural frequency of the primary system given by:

$$F(t) = 1.0 \times 10^4 \sin(\omega_n t). \tag{16}$$

There will be a resonance induced if there is no vibration absorber attached. Ideally if ω_n is already known, a linear oscillator can be designed to completely suppress the

vibration of the primary mass. But if ω_n is unknown or drifting, one has to employ an adaptive vibration absorber. As indicated in Ref [15], the performance of adaptive vibration absorbers are not as good as idealized linear oscillators for a vibration with a specified frequency, and the vibration of the primary block might not be able to be suppressed completely [15]. For vibration tuning, the SMA absorber is employed here, with its parameters as listed in Table (1), and its temperature chosen as $\theta = 347K$.

The simulation results with this temperature for vibration absorbing are presented in Figure (3). Because we are interested in "steady" vibrations, the displacement x_p and x_a are only plotted on the last one fourth of the whole simulated interval, which is $[7.5, 10]s$, in sub-plot (a) and (b), respectively. It is shown clearly that the attached block has a much larger amplitude than that of the primary block, which indicates that most of the vibration energy is absorbed by the attached oscillator. The vibration amplitude of the primary block is around $0.02m$, which is less than one tenth of that of the attached block. A discrete Fourier transformation is done on the simulated displacement of the SMA oscillator, and its spectrum is presented in the sub-plot (c), which indicates that the response of the SMA oscillator with the current temperature can be approximated very well by a linear oscillator because it has the same frequency response as linear oscillators. For clarification, the constitutive relation accounting for the force-deformation relation of the SMA rod is also plotted in the sub-plot (d), which indicates also a linear-like relation.

It is worth to note that the technique we used to estimate the temperature for the SMA absorber for a given excitation frequency is based on the equivalent stiffness of the SMA rod. Calculation according to Equation (14) indicates that when $\theta = 350K$, the SMA rod will have an equivalent stiffness 3.2×10^4 which gives a natural frequency $80 rad/s$. Because this is a nonlinear system, the estimated equivalence stiffness depends on the chosen deformation range which is influenced by other parameters like m_a, etc. Therefore, for a better performance, the temperature of the SMA absorber should be slightly adjusted around the estimated temperature according to the equivalent stiffness. For the current example, a few times of try-and-modify iterations using numerical simulations can lead us to an improved temperature value $\theta = 347K$.

To validate the SMA oscillator as an adaptive vibration absorber, the stiffness of the spring in the primary system is changed to $k_p = 100^2 m_p$, so its natural frequency becomes 100rad/s, and the frequency of the excitation is changed to $100 rad/s$ as well. For the vibration absorbing using the SMA oscillator, its temperature is estimated around $\theta = 403K$, at which its equivalent stiffness is $K_e = 5 \times 10^4 N/m$ and yields a natural frequency $100 rad/s$ for the SMA oscillator. A few try-and-modify iterations show that $\theta = 396K$ is an improved temperature. The displacement of the primary mass is sketched in a similar way in part (a) of Figure (4), and the frequency response of the absorber is plotted in part (b). It is shown that the vibration amplitude is very small, which indicates that the performance of the absorber is very good at this temperature. This can be explained by the fact that the SMA behaviour more like a linear spring at high temperature, which is also indicated in the frequency response
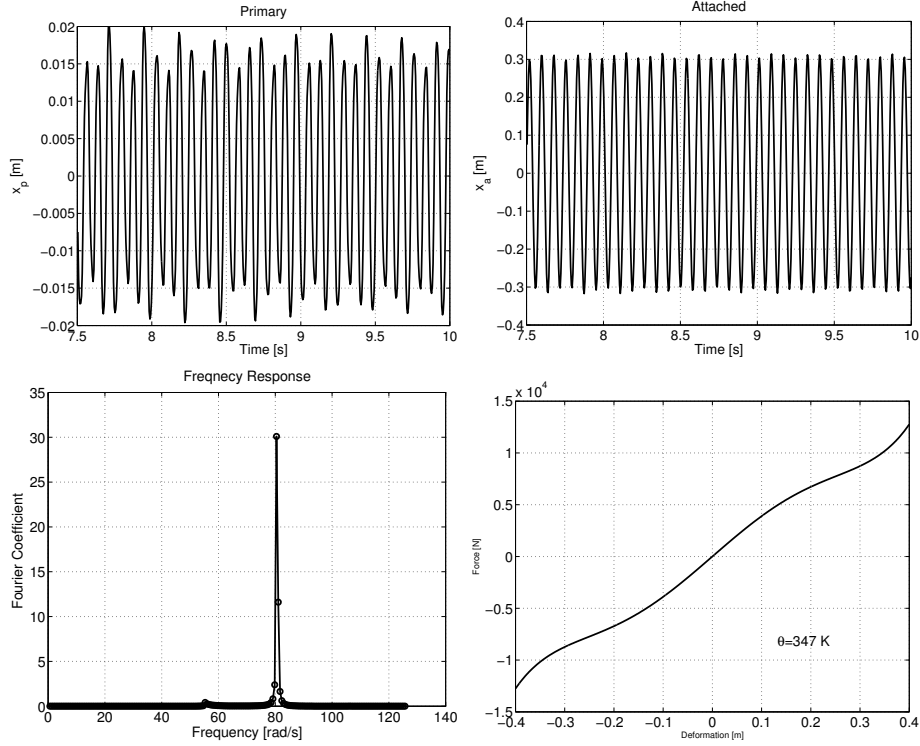
Figure 3: Numerical simulation of vibration absorbing using a shape memory alloy oscillator. From left to right, top to bottom, (a) displacement of the primary mass block, (b) displacement of the attached mass block, (c) frequency response of the absorber, (d) force-deformation relation of the absorber.

plotting.

For more comparison, the frequency of the primary system and excitation is changed to $65 rad/s$, and all other conditions are kept unchanged. For this case, the temperature of the SMA absorber is estimated to be $\theta = 282K$, for which numerical results are sketched in the same way in Figure (4) in part (c) and (d) for x_p and frequency response, respectively. It is shown that the amplitude of x_p is still successfully reduced to a very small value, the behaviour of the absorber is still similar to linear absorbers.

In the above numerical simulations, the SMA oscillator is working at high temperature, which means that the SMA rod is in the austenite phase and no hysteresis is observed. To exploit the application potential of the hysteresis due to phase transformations in the SMA rod, the oscillator is simulated finally with low temperature $\theta = 210K$. Due to the non-convex force-deformation relation with this temperature, as sketched in Figure (2), part (a), it is not reasonable to estimate its equivalent stiffness. Here, the numerical simulation is carried out to show the general vibration attenuation of the SMA oscillator at low temperature, without considering any specific frequencies. The friction force in the primary system is set to zero ($c_p = 0$), and frequency is adjusted to $\omega_n = 120 rad/s$ by changing k_p accordingly, and the excitation
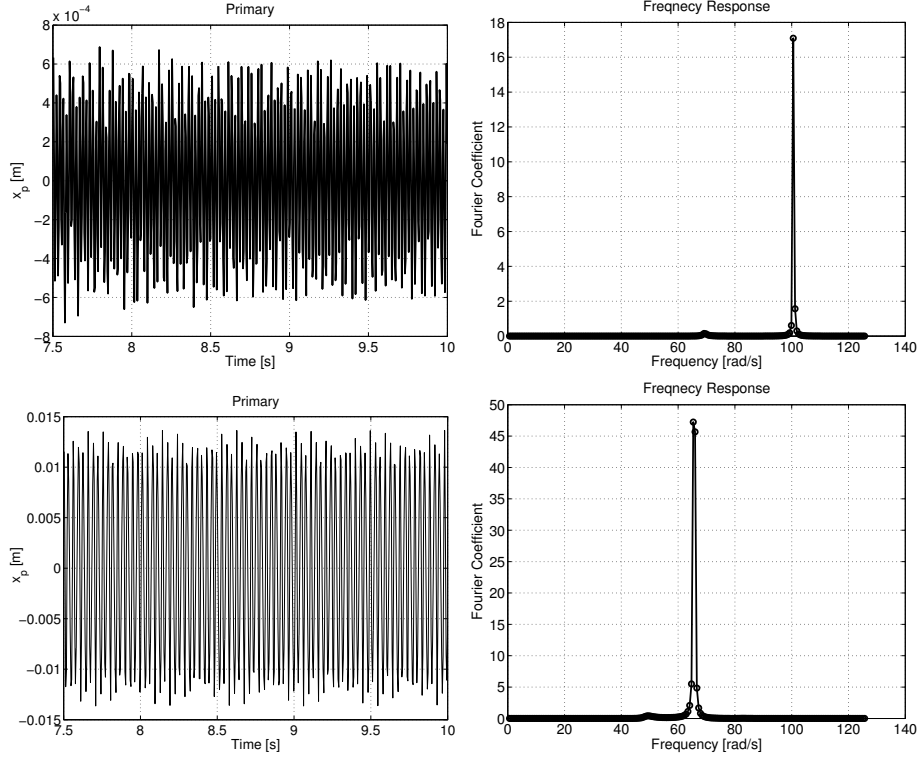
10

Figure 4: Numerical simulation of the adaptivity of SMA vibration absorber. From left to right, top to bottom, (a) Displacement of the primary mass, $\theta = 396K$. (b) Frequency response of the absorber, $\theta = 396K$. (c) Displacement of the primary mass, $\theta = 282K$. (d) Frequency response of the absorber, $\theta = 282K$.

is changed to the following switching function:

$$F(t) = 1.0 \times 10^4 \text{sign}(\sin(\omega_n t)), \tag{17}$$

where the function $\text{sign}(\cdot)$ has value 1 if the variable is positive and -1 if it is negative. The numerical simulations are sketched in Figure (5).

The amplitudes of x_p and x_a show that the major part of the energy is absorbed by the oscillator because the later has a larger amplitude. If the temperature is sustained at a low value, the vibration energy in the SMA oscillator will be continuously dissipated to make the vibration of the primary system attenuated [8, 11]. But the amplitude of x_p is obviously much larger than those results in the above simulations. These facts show that the performance of the SMA absorber at low temperature is not very satisfactory, but very robust when the excitation is not harmonic and unknown. The frequency response is much more complicated in this case, because the nonlinearity in the force-deformation becomes dominant at this temperature. In this case, a linear spring model loses its validity.

In all the above numerical simulations, the vibrations of the primary mass block are successfully attenuated by using the SMA absorber. Since the force-deformation
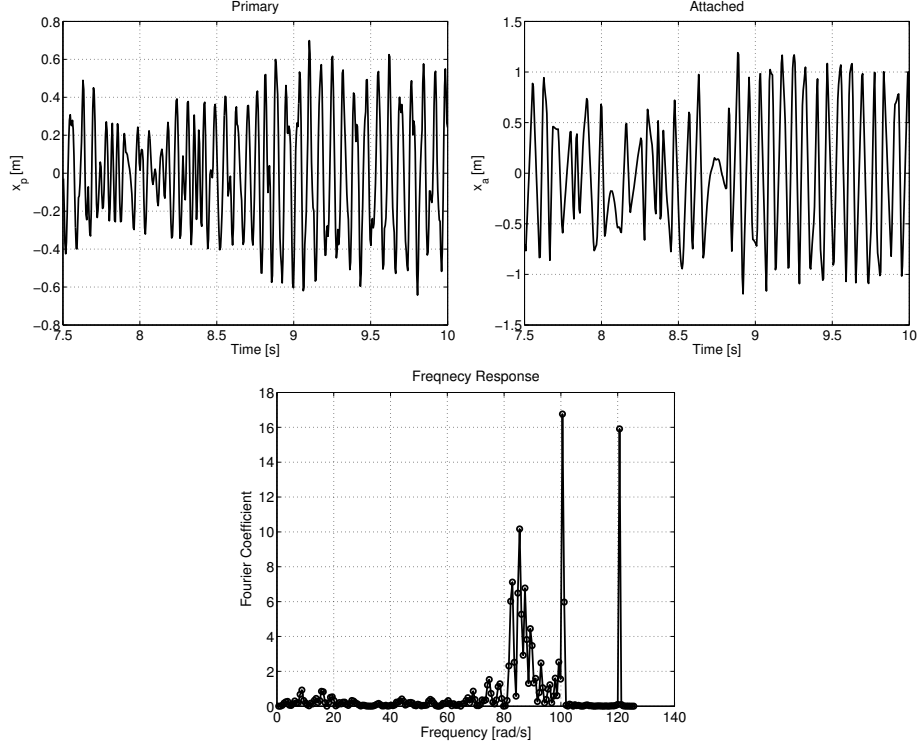
Figure 5: Numerical simulation of vibration absorbing using a shape memory alloy oscillator. From left to right, top to bottom, (a) Displacement of the primary mass; (b) Displacement of the attached mass; (c) frequency response of the absorber, (d) force-deformation of the absorber.

relation is nonlinear, the best temperature for vibration absorbing can be found by using standard optimization procedures. Here, we have implemented a simple technique to obtain a quick estimate for such a temperature.

5   Conclusion

In this paper, we modelled the performance of a SMA oscillator used as a vibration absorber. Two models for the SMA rod were used: first, we applied a partial differential equation based on the Ginzburg-Landau theory, and then we simplified this model to a nonlinear spring model, which is especially convenient for the vibration analysis. The latter model included thermo-mechanical coupling properties and hysteresis induced by phase transformations. Numerical simulations were carried out with various excitation frequencies. The results demonstrated that the SMA vibration absorber is adaptive, it can be adjusted to match different frequencies by changing its temperature. It has also been shown that the SMA absorber can be used as a general vibration attenuator when its temperature is low, making it a robust absorber when the frequency information about the primary system and excitation is unknown, or drifting.

References

[1] V. Birman, Review of mechanics of shape memory alloys structures, *Appl. Mech. Rev.* **50** (1997) 629-645.

[2] Y. C. Chen, D. C. Lagoudas, Impact induced phase transformation in shape memory alloys, *Journal of the Mechanics and Physics of Solids*, **48** (2000) 275 - 300.

[3] F. Falk, P. Konopka, Three-dimensional Landau theory describing the martensitic phase transformation of shape memory alloys. J.Phys.:Condens.Matter **2** (1990) 61-77.

[4] S.M.T. Hashemia, and S.E. Khademb, Modeling and analysis of the vibration behavior of a shape memory alloy beam, *Inter. Jour. Mech. Sci.* **48** (2006) 44-52.

[5] C.M. Harris, *Shock and Vibration Handbook*, 4thEdition, McGraw-Hill, New York, 1996.

[6] P. Kloucek, D. R. Reynolds, and T. I. Seidman, Computational modelling of vibration damping in SMA wires, *Continuum Mech. Thermodyn.* **16** (2004) 495 - 514.

[7] Katsuhiko Ogata, System Dynamics, 4th Edition. Pearson Education,Inc., 2004. New York.

[8] A. Masuda, and M. Noori, Optimisation of hysteretic characteristics of damping devices based on pseudoelastic shape memory alloys. *Inter. J. Nonlinear Mech.* **37** (2002) 1375-1386.

[9] M. C. Piedboeuf, R. Gauvin, and M. Thomas, Damping behaviour of shape memory alloys: Strain amplitude, frequency and temperature effects. *Journal of Sound and Vibration* **214** (5) (1998) 885 - 901

[10] E. Rustighi, M. J. Brennan and B. R. Mace, A shape memory alloy adaptive tuned vibration absorber: design and implementation, *Smart Materials and Structures*, **14** (2005) 19-28.

[11] S. Saadat, J. Salichs, M. Noori, Z. Hou, H. Davoodi, I. Bar-on, Y. Suzuki, and A. Masuda, An overview of vibration and seismic applications of NiTi shape memory alloy, *Smart Materials and Structures*, **11** (2002) 218-229.

[12] S. Sun, and R. K. N. D. Rajapakse, Simulation of pseudoelastic behaivour of SMA under cyclic loading, *Computational Materials Science* **23** (2003) 663 - 674.

[13] L. X. Wang, and R.V.N.Melnik, Dynamics of shape memory alloys patches, *Material Science and Engineering, A* **378** (2004) 470-474.

[14] K.A. Williams, G.T.-C. Chiu, and R.J. Bernhard, Passive adaptive vibration absorbers using shape memory alloys, *Proceedings of the SPIE*, Vol. **3668** (1999) 630 641.

[15] K. A. Williams, G. T. C. Chiu, and R. J. Bernhard, Dynamic modelling of a shape memory alloy adaptive tuned vibration absorber. *Journal of Sound and Vibration* **280** (2005) 211-234.

Proceedings of the Eighth International Conference on Computational Structures Technology

Edited by B.H.V. Topping, G. Montero and R. Montenegro

This book contains the extended abstracts of the contributed papers presented at the Eighth International Conference on Computational Structures Technology, held in Las Palmas de Gran Canaria, Spain, 12-15 September 2006.

The full length papers are available in electronic format on the accompanying CD-ROM. The topics covered include:

- Damage, Robustness & Service-Life
- Steel and Composite Structures
- Probabilistic Approaches
- Tall Buildings
- Dynamics & Traffic Vibrations
- Constitutive & Material Modelling
- Viscoelastically Damped Structures
- Masonry Structures
- Fabric, Cable & Membrane Structures
- Composite & Adaptive Structures
- Steel Structures
- Reinforced Concrete Structures
- Aluminium Structures
- Structural Analysis & Re-Analysis

- Bridge Engineering
- Joints & Connections
- Plates & Shells
- FEM, DEM & BEM
- Iterative Solution Methods
- Meshless Methods
- Multiscale Methods
- Adaptivity & Errors
- Buckling & Post-Buckling
- Optimization
- Design Methods & Studies
- Seismic Engineering
- Composite Materials
- Piezoelectric Materials

A keyword and author index is provided both in this book and on the CD-ROM.

Proceedings of
The Eighth International Conference on
Computational Structures Technology

Civil-Comp Press

ISBN 1-905088-06-X   Book
ISBN 1-905088-07-8   CD-ROM
ISBN 1-905088-08-6   Set

COMPACT
diSC
DATA STORAGE

Edited by B.H.V. Topping, G. Montero and R. Montenegro
Las Palmas de Gran Canaria - Spain
12-15 September 2006